Emittance-Exchange-Based High Harmonic Generation Scheme for a Short-Wavelength Free Electron Laser

B. Jiang,[1,2] J. G. Power,[1] R. Lindberg,[1] W. Liu,[1] and W. Gai[1]

[1]*Argonne National Laboratory, 9700 South Cass Avenue, Argonne, Illinois 60439, USA*

[2]*Shanghai Institute of Applied Physics, CAS, Shanghai 201800, China*

(Received 29 July 2010; published 16 March 2011)

Generation of short-wavelength radiation by a free-electron laser using up-frequency conversion of an electron bunch density modulation is currently an area of active research. We propose a new scheme for producing the longitudinal electron bunch density modulation similar to the recently proposed echo-enabled harmonic generation but based on an emittance exchange beam line and a multislit mask. Beam line analysis and start-to-end simulation are presented.

DOI: 10.1103/PhysRevLett.106.114801 PACS numbers: 41.60.Cr, 29.27.−a

The development of free-electron lasers (FELs) capable of generating short-wavelength radiation in the ultraviolet and soft x-ray regions is an area of active research. Two promising approaches are self-amplified spontaneous emission FELs [1] and high-gain harmonic generation FELs [2]. However, both of them face some technical challenges. Self-amplified spontaneous emission radiation has rather poor temporal coherence and suffers from shot-to-shot fluctuations [3,4], while high-gain harmonic generation radiation has limited frequency up-conversion capability. To address the latter limitation, a cascaded high-gain harmonic generation scheme has been proposed to reach higher harmonics [5], but this approach is sensitive to timing jitter and requires high charge bunches [6].

Recently, an echo-enabled harmonic generation (EEHG) FEL scheme was proposed to generate radiation at unprecedented high harmonics of the seed laser. EEHG simulations were presented in Ref. [7], and a demonstration experiment was done at Stanford Linear Accelerator Center observing 4th harmonic radiations [8]. The EEHG scheme [see Fig. 1(a)] uses two modulators to generate the longitudinal electron bunch density modulation. In "*modulator 1,*" the bunch first passes through a laser-seeded undulator, where it acquires an energy modulation, and second it passes through an overbunched chicane to produce energy bands. "*Modulator 2*" then converts the energy bands into a longitudinal density modulation at high harmonics of the seed laser.

It has recently become apparent to the accelerator community that the emittance exchange (EEX) beam line is useful beyond its original application of exchanging emittance between the longitudinal and transverse planes. Quite generally, it transforms features from the transverse plane into the longitudinal plane (and vice versa) and therefore has been used in a variety of applications [9–13]. In the original proposal [9], the EEX beam line was used to approximately exchange a smaller longitudinal emittance with a larger transverse one to improve the self-amplified spontaneous emission performance. A modified scheme was found later [10] in which a full phase-space exchange can be generated. More recently, an EEX beam line was used to generate longitudinal bunch trains and longitudinally ramped bunches [12] from a transversely segmented bunch at the entrance to the EEX beam line. In this Letter, we propose to use an EEX beam line as a part of a scheme to generate short-wavelength radiation from an FEL. The scheme we propose is comparable to EEHG-FEL [Fig. 1(a)] except in the method it uses to generate the energy bands. Despite the similarities, this scheme may deviate from what is meant by "echo," so we call it the emittance exchange high-harmonic generation scheme (EEX-HHG).

The overall layout of the EEX-HHG scheme is shown in Fig. 1(b). An incident bunch is generated by the upstream accelerator (not shown), acquires energy bands when it passes through modulator 1 and obtains the longitudinal density modulation upon passing through modulator 2. Since modulator 2 is identical to Ref. [7], we focus most of our discussion on modulator 1, which consists of a multislit mask followed by an EEX beam line. We begin by presenting a single particle model of modulator 1 to give the reader a clear picture of the underlying physics and justify this with a full numerical model at the end of the Letter.

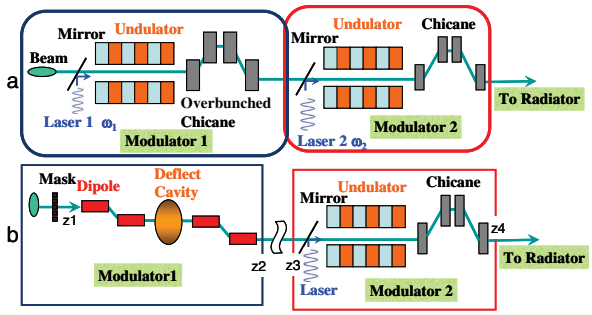

FIG. 1 (color online). Illustration of the EEHG-FEL scheme (a) and the EEX-HHG FEL scheme (b).

A multislit mask is used to segment the incident bunch into a series of beamlets separated in horizontal position at the entrance to the EEX beam line. The beamlets emerging from the mask are therefore distributed in a pattern of parallel lines and propagate into the EEX beam line. The dimensions of the metal slits can be quite challenging but nevertheless technically are achievable based on Ref. [14], and the heat load is negligible for typical repetition rates near 100 Hz.

The EEX beam line is used to transform particles initially separated in horizontal position into particles separated in energy at the exit. The beam line is composed of two dispersive sections (doglegs) with a rf deflecting cavity in between. Considering only the horizontal and longitudinal coordinates (x, x', z, δ), the transport matrix of the EEX beam line in the thick lens approximation can be found to be [11,13]

$$\begin{bmatrix} x_2 \\ x_2' \\ z_2 \\ \delta_2 \end{bmatrix} = \begin{bmatrix} 0 & L_c/4 & \left(\frac{L_c}{4}+L\right)k & -\frac{1}{k}+\left(\frac{L_c}{4}+L\right)k\xi \\ 0 & 0 & k & k\xi \\ k\xi & -\frac{1}{k}+\left(\frac{L_c}{4}+L\right)k\xi & \frac{L_c k^2 \xi}{4} & \frac{L_c k^2 \xi^2}{4} \\ k & \left(\frac{L_c}{4}+L\right)k & \frac{L_c k^2}{4} & \frac{L_c k^2 \xi}{4} \end{bmatrix} \begin{bmatrix} x_1 \\ x_1' \\ z_1 \\ \delta_1 \end{bmatrix}, \quad (1)$$

where the emittance exchange condition was used, namely, $1 + \eta k = 0$. L, η, and ξ are the length, dispersion, and momentum compaction of the dogleg, respectively, L_c is the length of the cavity, and $k = (eV_0)/(aE_0)$ is the cavity strength parameter. V_0 is the peak longitudinal rf voltage, $a = \lambda/\pi$, λ is the wavelength of the TM_{110}-like mode, and E_0 is the mean bunch energy.

The longitudinal distribution at the exit of EEX beam line depends on both the initial horizontal distribution and the EEX beam line according to Eq. (1) as

$$z_2 = k\xi x_1 + \left[-\frac{1}{k}+\left(\frac{L_c}{4}+L\right)\xi\right]kx_1' + \frac{L_c k^2 \xi}{4}(z_1 + \xi\delta_1), \quad (2)$$

$$\delta_2 = kx_1 + \left(\frac{L_c}{4}+L\right)kx_1' + \frac{L_c k^2}{4}(z_1 + \xi\delta_1), \quad (3)$$

where the subscripts 1 and 2 refer to the location before and after the EEX beam line, respectively. For the scheme considered in this Letter, our goal is to tune the incoming bunch phase space so that the final energy and position (δ_2, z_2) depend primarily on the initial horizontal position (x_1). The last term on the right-hand side of Eq. (2) and (3) can be forced to zero by tuning the initial energy chirp to

$$\delta_1/z_1 = -1/\xi, \quad (4)$$

where the upstream accelerator was used to place the chirp on the bunch. Next, the middle term in Eqs. (2) and (3) was made small in the following way. Given the EEX beam line parameters from Table I ($k = 2.9/\mathrm{m}$, $D = L_c/4 + L \approx 1$ m, and $\xi \approx -0.13$ m), then we need only to satisfy $Dx_1'/x_1 \ll 1$. Using the Twiss parameter formalism, we have $Dx_1'/x_1 = D\sqrt{\gamma/\beta} = D\sqrt{1+\alpha^2}/\beta$, and we can express our condition as one that the initial transverse correlation must satisfy:

$$D\sqrt{1+\alpha^2}/\beta \ll 1. \quad (5)$$

This can easily be satisfied if β is large compared to $D \bullet \alpha$. For our design we chose (see Table II) $\beta = 152$ m and $\alpha = 4$ so that $Dx_1'/x_1 = 0.03$. Incidentally, the large β function is not only useful for creating well separated energy bands but also places less of a burden on fabrication of the multislit mask since the slits can be farther apart.

Based on the above analysis we see that modulator 1 produces an energy modulated bunch by converting the horizontal position of the beamlets created by the mask (x_1) into an energy position created by the EEX beam line (δ_2). Moreover, if the injected bunch has the energy chirp of Eq. (4) and the transverse phase-space correlation of Eq. (5), then, by using Eqs. (2) and (3), the output bunch can be shown to have acquired a linear energy chirp

$$\delta_2/z_2 \approx 1/\xi, \quad (6)$$

which is useful for compressing the bunch length and hence increasing the bunch current for the FEL application.

We now briefly describe how modulator 2 converts the energy modulated bunch of modulator 1 into longitudinal density modulations containing high harmonics. A Fourier analysis of the longitudinal distribution of the bunch at the exit of modulator 1 shows that it is modulated by $\cos(2N\pi p)$. Here p is the normalized energy spread $p = (E - E_0)/\sigma_E$, σ_E is the energy spread of the bunch after

TABLE I. Modulator 1 parameters of the EEX-HHG design.

Total number of slits	25
Slit width/space	50/200 μm
Dogleg bend length	0.2 m
Drift space between bends	0.6 m
Bending angle	22°
Deflecting cavity length	0.2 m
Deflecting cavity strength k	2.9/m
Dispersion η	−0.35 m
Momentum compaction ξ	−0.13 m

TABLE II. Initial bunch parameters used in the simulation (data borrowed from the Fermi@elettra injector, with the exception of optimized bunch length and Twiss parameters).

Bunch energy	95 MeV
Bunch charge	0.8 nC
Normalized emittance (x/z)	1.5/3.7 μm
Bunch size, x (rms)	1.1 mm
Energy spread (uncorrelated/correlated)	2/ $\sim$ 150 keV
Bunch length	700 fs
β/α function	152 m/4.0

modulator 1, and N is the number of energy bands per σ_E. Approximating the energy distribution to be a smoothly varying sinusoidal, we have

$$f_0(p) = \frac{1}{\sqrt{2\pi}} e^{-p^2/2} \cos(2N\pi p). \quad (7)$$

By following the method used in Ref. [7], the energy and position coordinates (z, p) at the entrance to modulator 2 are converted by the laser-seeded undulator and the chicane to the coordinates $z' = z + (Bp/q)$, $p' = p + A\sin(qz)$, where $A = \Delta E/\sigma_E$, q is the laser wave number, and ΔE is the bunch energy modulation produced by the laser, $B = R_{56} q \sigma_E / E_0$, where R_{56} is the dispersive strength of the chicane. The final longitudinal phase-space distribution function after modulator 2 can be found:

$$f_1(p,z) = \frac{1}{\sqrt{2\pi}} e^{-[p - A\sin(qz - Bp)]^2/2} \times \cos\{2N\pi[p - A\sin(qz - Bp)]\}. \quad (8)$$

The longitudinal position distribution function is obtained by integrating $f_1(p, z)$ over p:

$$\rho(z) = \int_{-\infty}^{\infty} f_1(p)dp = \sum_{j=1}^{\infty} b_j \cos(jqz + \phi_j) + C, \quad (9)$$

where C represents the dc offset of the integral and b_j is the amplitude of the jth harmonic of the longitudinal distribution:

$$b_j \approx 2e^{-(Bj - 2N\pi)^2/2}(1 + e^{-4N\pi Bj})|J_j(2AN\pi)|. \quad (10)$$

The maximum value of this amplitude occurs when

$$j = \text{round}(2N\pi/B), \quad (11)$$

where the quantity round(n) denotes the integer nearest to n. Equation (11) shows that one can control the location of the radiation spectrum peak by adjusting N and B, but we note that these values are constrained by practical considerations such as N must be suitable for fabricating the mask, etc. For comparison purposes, the amplitude of the peak harmonic in the EEHG scheme [c_k in Eq. (8) of Ref. [7]] depends on the laser strength $A1$ which must be increased to create well separated energy bands while EEX-HHG relief.

As a practical example we carried out a study by using the initial bunch parameters from the Fermi@elettra injector [15]. In modulator 1, the beam dynamics simulation in the EEX beam line were performed with PARMELA (including space charge effects) [16], and MATLAB routines were written to handle the particle input/output at the mask and to apply the deflecting cavity thick lens matrix.

The bunch parameters from the Fermi@elettra injector are listed in Table II. The charge is reduced by the slits from 0.8 to 0.2 nC at location $z1$ in Fig. 1(b), as is the bunch current. The initial energy chirp was made to match the EEX energy chirp requirement [Eq. (4)]. The initial Twiss parameters were chosen to satisfy two conditions: (i) the initial transverse correlation must satisfy Eq. (5); and (ii) as explained in Ref. [17], the Twiss parameters must be chosen to avoid emittance dilution in the EEX beam line [see Fig. 2(a)].

The EEX beam line parameters are listed in Table I. The energy bands at the exit of modulator 1 are shown in Fig. 2(b), where the total rms energy spread is 0.23 MeV and the normalized transverse emittance is 5 mm mrad. Recall that the bunch emerging from modulator 1 is relatively easy to compress since it is already linearly chirped according to Eq. (6). Therefore, before entering modulator 2, we used a simple linear transformation to model the compression of the bunch by a chicane to 200 fs and acceleration to 1.2 GeV (not shown). The phase space corresponding to this point is shown in Fig. 2(c). Note that, since the scale of the total bunch length is much longer than that of the laser wavelength, only a small fraction of the bunch is sampled for the final phase-space plot after modulator 2 as indicated by the thin rectangular box in Fig. 2(c). The longitudinal phase space after modulator 2 of this sampled region is shown in Fig. 2(d). Finally, projecting the phase space along the z axis reveals tens of

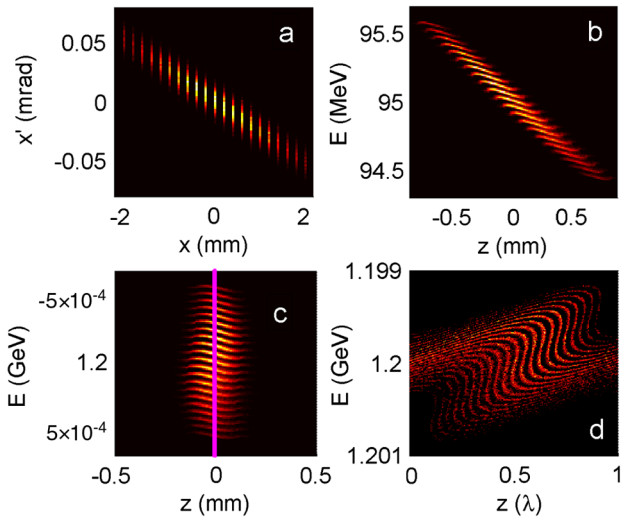

FIG. 2 (color online). Simulation results at different locations of the EEX-HHG beam line corresponding to the locations in Fig. 1: (a) bunch transverse phase space after mask at $z1$ in Fig. 1; (b) energy bands created by EEX at $z2$ in Fig. 1; (c) bunch after further acceleration and length compression at $z3$ in Fig. 1; (d) density modulation by modulator 2 at $z4$ in Fig. 1.

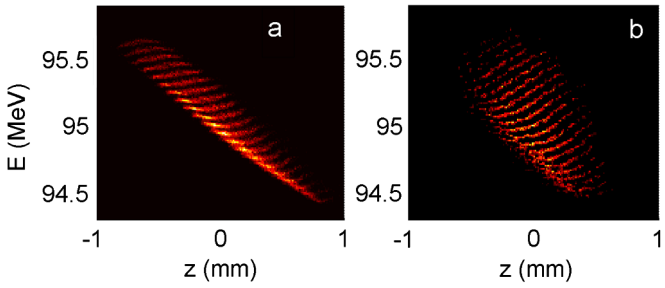

FIG. 3 (color online). CSR effect in EEX with different bending angles: (a) 22°; (b) 12°.

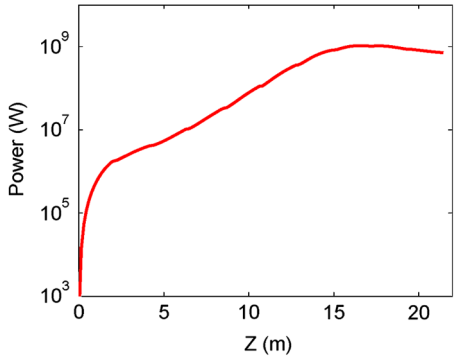

FIG. 4 (color online). FEL power evolution through the undulator.

spikes within one laser wavelength indicating the generation of very high harmonics.

To ensure the robustness of the EEX-HHG scheme, we examined whether coherent synchrotron radiation (CSR) could smear out the bands and degrade the production of high harmonics by using CSRTRACK [18]. Note that CSR was tracked only in the "doglegs" of the EEX section to compare it to the EEHG scheme [7]. Figure 3(a) shows the longitudinal phase space (with CSR) at the exit of the EEX. The induced energy spread (σ_{dE}) from CSR is 30 keV. Comparing the CSR result of Fig. 3(a) to that of Fig. 2(b), we see that the energy bands remain mostly intact. We repeated the CSR calculation in Fig. 3(b) for a smaller dogleg bending angle (smaller η), which shows even less smearing of the bands. The downside of a small bend angle, according to the emittance exchange condition ($1 + k\eta = 0$), is that it requires higher k, which places an additional burden on the deflecting cavity. In a real beam line design, a trade-off study would be made between CSR effects and the high-voltage capability of the deflecting cavity.

The final result was to send the density modulated bunch into the FEL by using GINGER [19] for the simulation. The radiator beam line consists of several sequential focusing-defocusing quadrupoles sections, and each sequential focusing-defocusing quadrupoles section has two 2.01-m-long, 3-cm-period undulators and two quadrupole-drift lines. By using a 400-nm seed laser, radiation power at the 24th harmonic (16.67-nm wavelength) is plotted in Fig. 4, which shows that the power saturated at an undulator length of 16.5 m and 1 GW of peak power.

In summary, when the EEX-based energy-band generation scheme is combined with modulator 2, high harmonics of the seed laser can generate ultraviolet radiation. It is also possible (albeit more challenging) to obtain soft x-ray radiation by using this scheme with a shorter-wavelength seed laser and a correspondingly smaller slit mask. A secondary benefit of the EEX-based scheme is that it will generate a small transverse emittance provided the initial longitudinal emittance of the injected bunch is small. We have shown that CSR does not wash out the energy bands. Particle loss at the mask causes a reduction in current, but due to the linear energy chirp the bunch length can be compressed to restore the high peak bunch current needed by the FEL lasing condition.

The authors thank K. J. Kim for many useful discussions. This work was supported by the U.S. Department of Energy under Contract No. DE-AC02-06CH11357 with Argonne National Laboratory.

[1] R. Bonifacio, C. Pellegrini, and L. M. Narducci, Opt. Commun. **50**, 6 (1985).
[2] L. H. Yu, Phys. Rev. A **44**, 5178 (1991).
[3] K.-J. Kim, Nucl. Instrum. Methods Phys. Res., Sect. A **250**, 396 (1986).
[4] J. M. Wang and L. H. Yu, Nucl. Instrum. Methods Phys. Res., Sect. A **250**, 484 (1986).
[5] Juhao Wu and L. H. Yu, Nucl. Instrum. Methods Phys. Res., Sect. A **475**, 104 (2001).
[6] L. H. Yu, Report No. BNL-71229-2003-IR, 2003.
[7] G. Stupakov, Phys. Rev. Lett. **102**, 074801 (2009).
[8] D. Xiang *et al.*, Phys. Rev. Lett. **105**, 114801 (2010).
[9] M. Cornacchia and P. Emma, Phys. Rev. ST Accel. Beams **5**, 084001 (2002).
[10] K.-J. Kim and A. Sessler, AIP Conf. Proc. **821**, 115 (2006).
[11] P. Emma *et al.*, Phys. Rev. ST Accel. Beams **9**, 100702 (2006).
[12] Y.-E. Sun *et al.*, Phys. Rev. Lett. **105**, 234801 (2010).
[13] Y.-E. Sun *et al.*, in *Proceedings of PAC07, Albuquerque, New Mexico, 2007* (IEEE, New York, 2007), pp. 3441–3443.
[14] N. Delerue *et al.*, in *Proceedings of PAC09, Vancouver, Canada, 2009* (IEEE, New York, 2009), paper TH5RFP065.
[15] C. J. Bocchetta *et al.*, ELETTRA Report No. ST/F-TN-07/12, 2007.
[16] J. H. Billen and L. M. Young, PARMELA Reference Manual, Report No. LA-UR-96-1835, 2000.
[17] M. Rihaoui *et al.*, AIP Conf. Proc. **1086**, 279 (2009).
[18] M. Dohlus, A. Kabel, and T. Limberg, Nucl. Instrum. Methods Phys. Res., Sect. A **445**, 338 (2000).
[19] W. M. Fawley, Lawrence Berkeley National Laboratory Report No. LBNL-49625-Rev.1, 2004.